NUMERICAL INVESTIGATION OF SURFACE REGRESSION EFFECTS ON INTERFERENCE GENERATED FLOW PATTERNS INSIDE LIQUID DROPLETS

Edson G. Moreira Filho[♦]- edson@lmt.coppe.ufrj.br
Albino J.K. Leiroz[♠] - leiroz@ime.eb.br
Department of Mechanical and Materials Engineering
Instituto Militar de Engenharia
22290-270 - Rio de Janeiro, RJ, Brazil

Abstract. A numerical study of droplet surface regression effects on the interference generated flow patterns within the liquid-phase of an infinite linear array of spherical droplets in the absence of surrounding convective effects is discussed in the present work. The transient evolution of the flow field, obtained using an axisymmetric vorticity-stream function approach, show the development of two toroidal vortices surrounded by a viscous boundary layer close the liquid-gas interface and by a internal wake in the stream axis region. The evolution of the temperature field is also analyzed. An analytical grid generation procedure is used in order to transform the moving-boundary physical domain into a fixed-boundary computational domain and to cluster points in the droplet surface near field, where pronounced gradients are expected. The transformed equations are discretized using the Finite Difference Method and the resulting system of algebraic equations is solved by iterative methods with local error control. Results indicate that velocity and temperature distribution inside individual stream droplets are significantly different from patterns found for isolated droplets in convective streams. Besides, comparison with results where the droplet surface regression is neglected show that the flow and temperature field developments are delayed by the moving boundary effect.

Keywords: Droplet Combustion, Droplet Vaporization, Numerical Methods, Convection, Moving Boundary.

1. INTRODUCTION

The atomization of liquid fuel jets, which usually precede the vaporization and combustion in a wide range of important technological applications, invariably leads to sprays with a large droplet volumetric fraction. Within these dense sprays, interaction effects and deviations from the isolated droplet behavior (Spalding, 1953; 1955) become significant and the multi-dimensionality of the phenomena makes pure analytical treatments not applicable.

Reviews of numerical studies of multi-droplet combustion have been presented covering a broad selection of physical situations and stressing the importance of droplet interaction (Sirignano, 1993, Annamalai, 1992). Numerical studies share the compromise of addressing the

---

[♦] Currently at the Mechanical Engineering Program/COPPE of the Federal University of Rio de Janeiro (UFRJ).
[♠] Author to whom correspondence should be addressed.

different spatial and time scales present in the multi-droplet combustion phenomena and are usually limited to arrays with a small number of droplets.

The droplet interaction phenomena can be understood from the nature of the involved physical process. Energy in the form of heat diffuses and convects from the surrounding ambiance or reaction zone to the droplet surface, increasing the liquid droplet temperature and leading to phase-change. Mass diffusion is also present due to species concentration gradients. In a combustion situation, the vaporized liquid is transported to the flame (Stefan Flow) where reaction occurs and heat is released to the ambient and to the condensed phase. Interdroplet effects alter the manner in which an individual droplet receives heat and thus affect its heating and vaporization process. In reacting situations, competition for the ambient oxidant affect the flame position and shape, and variations in ignition delays become influenced by the spray denseness.

Liquid circulation studies for isolated droplets in convective streams show the development of a single toroidal vortex surrounded by a viscous boundary layer and an internal wake (Prakash & Sirignano, 1978). Liquid vaporization effects are initially neglected. Results are used to correlate the vortex strength to the shear stress at the liquid-gas interface. Energy diffusion within the recirculation zone is also shown to follow a one-dimensional behavior due to the circulatory flow pattern. For vaporizing liquid droplets, an integral approach is used in the analysis of the viscous, thermal and species boundary layers (Prakash & Sirignano, 1980). Results show the importance of transient effects and that the temperature distribution within the discrete phase is nonuniform during the droplet lifetime.

A detailed numerical analysis of a spherical droplet suspended by a thin filament in a convective stream (Shih & Megaridis,1995). The filament suspended droplet is a typical setup for reactive and nonreactive experimental studies. Results show the influence of filament on the general liquid internal circulation, which includes the development of secondary vortices. Besides, significant effects of the circulation patterns on the droplet vaporization rate were observed.

In the absence of convective effects, droplet mass vaporization reduction in linear reacting arrays due to interference was found and correlated to interdroplet spacing (Leiroz & Rangel, 1995a; 1995b). Furthermore, the nonconvective quasi-steady results indicate the potential flow solution as a valid approximation for the viscous velocity field, based on a negligible tangential velocity observed along the droplet surface. The droplet surface blowing velocity was found the vary along the liquid-gas interface leading to the observed negligible tangential velocity.

Gas-phase transient results during droplet stream combustion have shown the existence of non-vanishing droplet surface tangential velocities that can lead to shear-induced liquid motion within the dispersed phase (Leiroz, 1996). Nevertheless, similarly to the quasi-steady case, the droplet surface normal velocity was found to vary along the liquid-gas interface. Besides, preferential vaporization near the droplet equatorial plane, that can also induce liquid movement inside the droplet, was also observed. Results also show, for the time intervals investigated, a weak dependence of the droplet mass vaporization rate on the interdroplet spacing.

In the present work, the effect of droplet surface regression on the transient motion of liquid inside spherical droplets generated by the presence of significant interference effects in droplet streams under stagnant environment conditions is numerically investigated. Constant thermophysical properties are assumed for the purpose of the calculations. The droplet surface normal velocity dependence on the angular position is neglected for the present work. The transient energy and momentum governing equations, written in vorticity-stream function formulation, are discretized using the BTCS Finite Difference scheme (Hoffman, 1992). Results show the temporal evolution of the flow and temperature fields, which are initially compared with patterns found in isolated droplet in convective conditions. Comparisons with results obtained neglecting the droplet surface regression (Moreira Filho & Leiroz, 2000) indicate a delay on the flow and temperature field development for the same conditions.

2. ANALYSIS

In the absence of external convective effects, the study of interactive effects within the dispersed phase of a infinitely long linear array of spherical equidistant droplets, shown in Fig.1a can be performed in the solution domain depicted in Fig.1b. Symmetry considerations around the droplet stream axis, the droplet equatorial plane and the interdroplet mean distance plane are explored in the simplification of the solution domain.

The flow and energy governing equations are written in nondimensional form, assuming constant thermophysical properties, negligible body forces and secondary convective effects, as
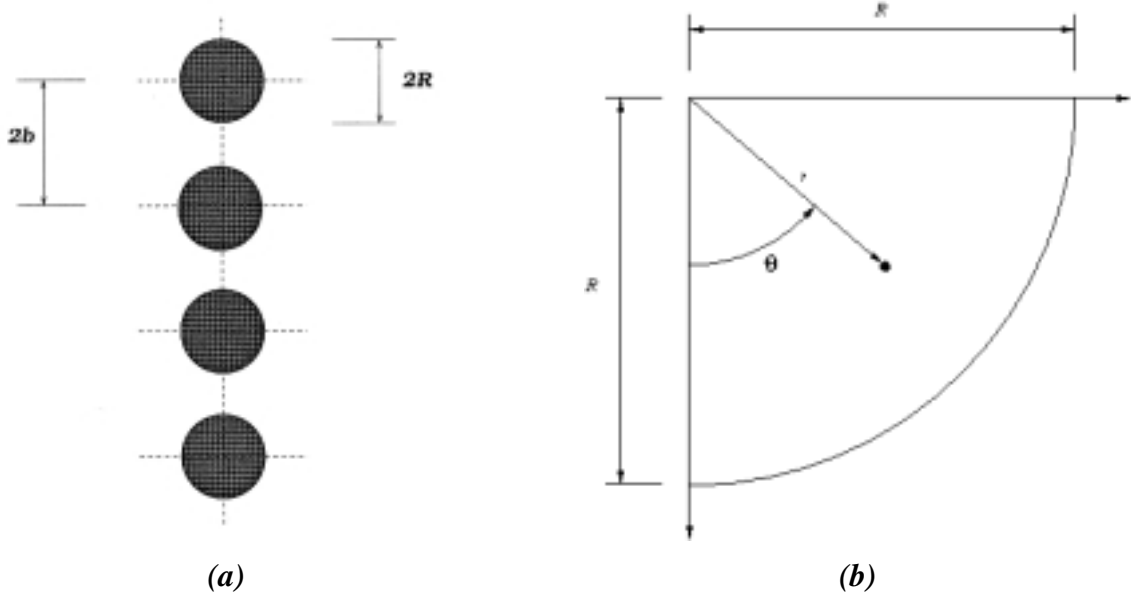

(a)   *(b)*

Figure 1. Sketch of the center portion of an infinite stream of droplets *(a)* and physical domain and principal dimensions *(b)*

$$\frac{1}{r^2}\frac{\partial}{\partial r}\left(r^2 u_r\right) + \frac{1}{r\,sin\theta}\frac{\partial}{\partial\theta}\left(u_\theta\,sin\theta\right) = 0 \tag{1}$$

$$\frac{\partial u_r}{\partial t} + u_r\frac{\partial u_r}{\partial r} + \frac{u_\theta}{r}\frac{\partial u_r}{\partial\theta} - \frac{u_\theta^2}{r} = -\frac{\partial p}{\partial r} +$$
$$\frac{1}{Re_o}\left[\frac{1}{r^2}\frac{\partial^2}{\partial r^2}\left(r^2 u_r\right) + \frac{1}{r^2\,sin\theta}\frac{\partial}{\partial\theta}\left(sin\theta\frac{\partial u_r}{\partial\theta}\right)\right] \tag{2}$$

$$\frac{\partial u_\theta}{\partial t} + u_r\frac{\partial u_\theta}{\partial r} + \frac{u_\theta}{r}\frac{\partial u_\theta}{\partial\theta} + \frac{u_\theta u_r}{r} = -\frac{1}{r}\frac{\partial p}{\partial\theta} +$$
$$\frac{1}{Re_o}\left[\frac{1}{r^2}\frac{\partial}{\partial r}\left(r^2\frac{\partial u_\theta}{\partial r}\right) + \frac{1}{r^2}\frac{\partial}{\partial\theta}\left(\frac{1}{sin\theta}\frac{\partial(u_\theta\,sin\theta)}{\partial\theta}\right) + \frac{2}{r^2}\frac{\partial u_r}{\partial\theta}\right] \tag{3}$$

$$\frac{\partial T}{\partial t} + u_r\frac{\partial T}{\partial r} + \frac{u_\theta}{r}\frac{\partial T}{\partial\theta} = \frac{1}{Pe_o}\left\{\frac{1}{r^2}\frac{\partial}{\partial r}\left(r^2\frac{\partial T}{\partial r}\right) + \frac{1}{r^2\,sin\theta}\frac{\partial}{\partial\theta}\left(sin\theta\frac{\partial T}{\partial\theta}\right)\right\} \tag{4}$$

with boundary conditions

$$u_\theta = u_{\theta,s}(\theta)\,,\ u_r = u_{r,s}(\theta)\,,\ T = 1\,;\ r = R(t)\,,\ 0 < \theta < \pi/2 \tag{5}$$

$$u_\theta = 0\,,\ \frac{\partial u_r}{\partial \theta} = 0\,,\ \frac{\partial T}{\partial \theta} = 0\,;\ \theta = 0\,,\ 0 \le r \le R(t) \tag{6}$$

$$u_\theta = 0\,,\ \frac{\partial u_r}{\partial \theta} = 0\,,\ \frac{\partial T}{\partial \theta} = 0\,;\ \theta = \pi/2\,,\ 0 \le r \le R(t) \tag{7}$$

and initial conditions

$$u_\theta = 0\,,\ u_r = 0\,,\ T = 0\,;\ 0 \le r \le 1,\ 0 \le \theta \le \pi/2 \tag{8}$$

which corresponds to the instantaneous injection of the droplet stream into an surrounding gas environment.

The nondimensional variables in Eqs. 1-8 are defined as

$$r = \frac{r^*}{R_o}\,;\ u_\theta = \frac{u_\theta^*}{u_{s,max}^*}\,;\ u_r = \frac{u_r^*}{u_{s,max}^*}\,;\ p = \frac{p^*}{\rho(u_{s,max}^*)^2}\,;\ t = \frac{t^*}{R_o / u_{s,max}^*}\,;\ T = \frac{T^* - T_0^*}{T_s^* - T_0^*} \tag{9}$$

where the initial droplet radius (R_o) and the maximum tangential velocity along the droplet surface $(u_{s,max}^*)$ are used as length and velocity characteristic quantities, respectively.

According to the nondimensional variables defined in Eq. 9, the Reynolds (Re_o), Prandtl (Pr) and Peclet (Pe_o) numbers are defined as

$$Re_o = \frac{u_{s,max}^* R_o}{\nu}\,;\ Pr = \frac{\nu}{\alpha}\,;\ Pe_o = Re_o \cdot Pr \tag{10}$$

where ν and α represent the kinematic viscosity and the thermal diffusivity, respectively.

In order to decouple the pressure and velocity fields and reduce the number of equations necessary for the flow analyses, the primitive variable formulation described by Eqs. 1-3 are rewritten in vorticity-stream function form as

$$\frac{\partial \xi_\phi}{\partial t} + u_r \frac{\partial \xi_\phi}{\partial r} + \frac{u_\theta}{r} \frac{\partial \xi_\phi}{\partial \theta} =$$
$$\frac{\xi_\phi}{r}(u_r + u_\theta \cot\theta) + \frac{1}{Re_o}\left\{ \frac{1}{r^2} \frac{\partial}{\partial r}\left(r^2 \frac{\partial \xi_\phi}{\partial r} \right) + \frac{1}{r^2} \frac{\partial}{\partial \theta}\left[\frac{1}{\sin\theta} \frac{\partial}{\partial \theta}(\xi_\phi \sin\theta) \right] \right\} \tag{11}$$

$$-\xi_\phi = \frac{1}{r^2 \sin\theta} \frac{\partial}{\partial r}\left[r^2 \frac{\partial}{\partial r}\left(\frac{\psi}{r} \right) \right] - \frac{1}{r^3} \frac{\partial}{\partial \theta}\left[\frac{1}{\sin\theta} \frac{\partial \psi}{\partial \theta} \right] \tag{12}$$

with boundary conditions

$$\frac{\partial \psi}{\partial \theta} = u_{r,s}(\theta) r^3 sin(\theta); \ r = R(t), \ 0 < \theta < \pi/2 \tag{13}$$

$$\psi = 0, \ \xi_\phi = 0; \ \theta = 0, \ 0 \le r \le R(t) \tag{14}$$

$$\psi = 0, \ \xi_\phi = 0; \ \theta = \pi/2, \ 0 \le r \le R(t) \tag{15}$$

and initial conditions

$$\psi = 0, \ \xi = 0; \ 0 \le r \le 1, 0 < \theta < \pi/2 \tag{16}$$

Vorticity (ξ_ϕ) and stream function (ψ) are respectively defined by the radial and tangential velocity components as

$$\xi_\phi = \frac{1}{r} \frac{\partial}{\partial r}(r u_\theta) - \frac{1}{r} \frac{\partial u_r}{\partial \theta} \tag{17}$$

and

$$u_r = \frac{1}{r^2 sin\theta} \frac{\partial \psi}{\partial \theta}; \ u_\theta = -\frac{1}{r sin\theta} \frac{\partial \psi}{\partial r} \tag{18}$$

The vorticity value at the liquid-gas interface is initially unknown and is determined by an iterative solution procedure of Eqs.10-15, which also accounts for the treatment of the non-linear terms present in Eq.10.

3. NUMERICAL CONSIDERATIONS

In order to improve solution convergence and control computational costs, clustering of points in the radial direction close to the liquid-gas interface is introduced. The clustering of points is motivated by the high solution gradients expected close to the droplet surface. During the grid generation procedure, an analytical transformation expressed by (Anderson *et al.*, 1984)

$$\eta = 1 + \frac{1}{\tau} sinh^{-1}[(r-1)sinh(\tau)] \tag{19}$$

is applied, where the clustering parameter τ allows the control of the radial point distribution. Analytically obtained metrics are used to rewrite Eqs. 4, 11 and 12, using the introduced transformed variable η.

The numerical treatment of the droplet surface regression is also achieved by the introduction of an analytical transformation of variables expressed by (Rangel & Bian, 1995)

$$\Gamma = R_o t \tag{20}$$

$$w(t) = \frac{4}{\pi} tan^{-1}\left(\frac{\eta}{\eta_s(t)}\right) \tag{21}$$

where $\eta_s(t)$ corresponds to the instantaneous position of the droplet surface. Due to the singularity present in Eq.21 for $\eta_s(t)=0$, numerical calculations are performed until the droplet size is reduced to a predefined value.
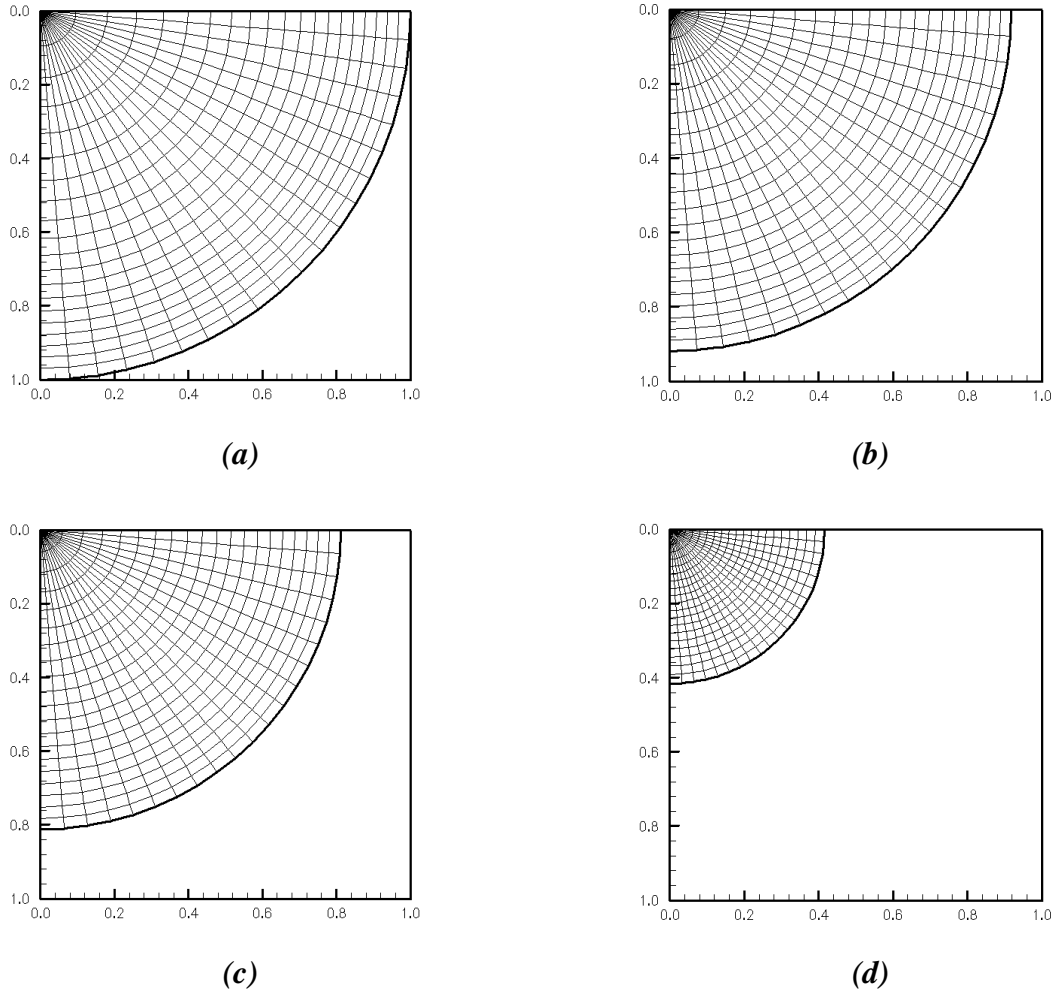

(a)

(b)

(c)

(d)

Figure 2: Discretizing grid in the physical domain for $\tau = 2.5$, 21×21 points and $u_r = 10^{-3}$ – *(a) t=0, (b) t=0.2, (c) t=0.4, (d) t=0.8.*

The transformed equations are discretized into algebraic form using a BTCS Finite-Difference scheme (Anderson *et al*., 1984). The resulting system of algebraic equation is solved by iterative methods with local error control. Once convergence is achieved, Eq.19-21 are analytically inverted and the solution profiles within the physical domain are obtained. Discretizing grids within the physical domain are depicted in Fig.2 for different times. Regularly spaced grids are recovered for vanishing clustering parameters values. For the present work, the dependence on the angular position of the velocity tangential component along the droplet surface is obtained from gas-phase transient calculations (Leiroz, 1996).

4. RESULTS

The developed numerical procedure was initially validated for the limiting case of an isolated droplet for which the transient droplet surface velocity induced by interference vanishes. An analytical solution for the energy equation is obtained neglecting the convective terms. A

convergence study is also performed in order to calibrate the mesh parameter τ. For the present work, the functional dependence of the droplet surface tangential velocity is obtained from gas-phase calculations. In order to evaluate the droplet surface regression effect, an artificially small droplet blowing velocity is used. For the results shown in the present work $u_{\theta,s} = sin(2\theta)$ and $u_r = 10^{-5}$. Simulations were conducted on *126×126* grids for a tolerance of 10^{-4}, a clustering parameter τ equal to *2.5* and $\Delta t = 10^{-4}$ which allow a 3-digit precision on the depicted results.
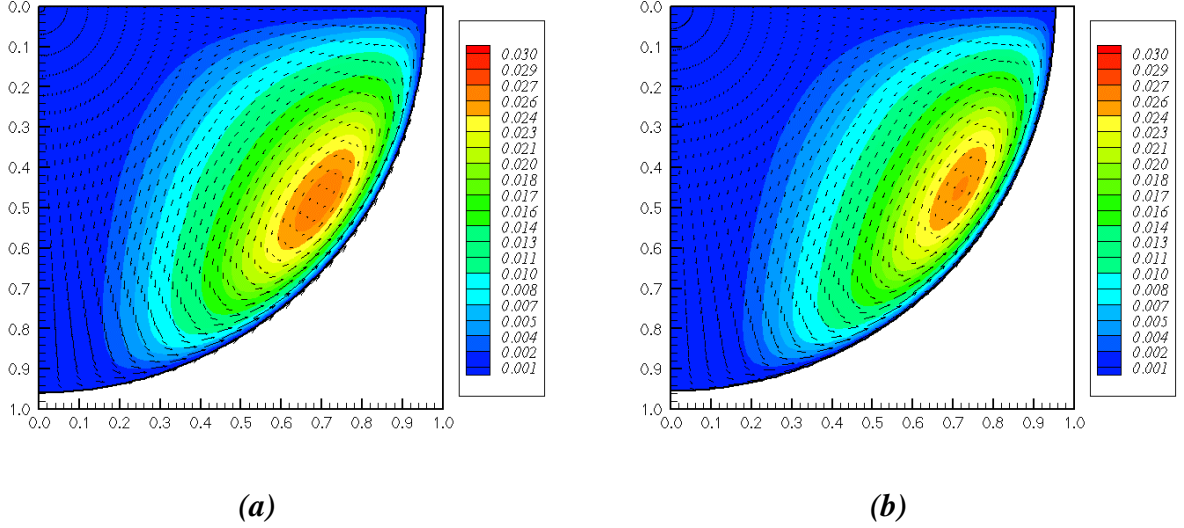
Figure 3. Stream-function and velocity vectors for $t = 1$, $Re_o = 10$ *(a)* and $Re_o = 100$ *(b)* – 126×126 grid, $\tau = 2.5$, $u_{\theta,s} = sin(2\theta)$, $u_r = 10^{-5}$

Stream-function transient results are shown in Fig.3 for $t = 1$, $Pr = 10$ and different Reynolds numbers indicate the existence of two toroidal vortices within the liquid phase separated by the droplet equatorial plane. More intense stream-function gradients are observed as the Reynolds number *(Re$_o$)* increases. A displacement of the vortex center towards to droplet equatorial plane is also observed for higher *(Re$_o$)*. The existence of a boundary layer close to the liquid-gas interface and of a wake between the vortex and the droplet stream axis is also observed. Although these structures are also present in the flow pattern found for isolated droplets in convective stream (Prakash & Sirignano, 1978), the calculated two-vortex pattern is significantly different from the single vortex found for that configuration. Also, results can be used to quantify the vortices strength. The liquid motion effect on the droplet stream transport mechanisms is currently under study. Moreover, a comparison with results obtained neglecting the droplet surface movement (Moreira Filho, 2000) show, for the surface regression case, a *50%* reduction of stream-function values. This difference indicate that, for the conditions studied, vaporization delays the development of the flow field. For latter times, the dependence of the stream-function results on the Re_o is weakened and a reduction of the stream-function calculated values is also observed, as shown in Fig.4 for $t = 3$. It should also be mentioned that steady-state results are obtained for $t = 2$ if the regression of the liquid-gas interface is neglected.

The evolution of the temperature field is depicted in Fig.5 for $Re_o = 10$ and $Re_o = 100$. The Prandtl number *(Pr)* equal to *10*, which is a typical value for liquid fuels, is considered. For initial times, the development of the temperature field presents a weak dependence on the angular position within the liquid droplet as shown in Fig.5a for $t = 2$. Despite the almost diffusive behavior associated with early stages of the flow development, a broadening of the thermal boundary layer close to the droplet equatorial plane is observed in Fig. 5b for $Re_o = 100$. For Re_o

equal to *10* a similar quasi-radial behavior of the temperature field is observed as shown in Figs. 5c and 5e for $t = 4$ and *6*, respectively. Results obtained neglecting the droplet surface regression indicate for $Re_o = 10$ a significant deviation from the quasi-radial profiles during the droplet lifetime that leads to a more pronounced temperature field development. The lagging on the temperature field development when droplet vaporization is considered is caused by the weakening of the convective effects due to the mass flow across the droplet surface. For *Re = 100* the development of the temperature field is influenced by convective effects and a departure from the quasi-radial behavior becomes significant as shown in Figs. 5d and 5f. The inward motion of fluid observed as θ approach $\pi / 2$ is responsible for the preferential temperature field development. Qualitatively, the temperature fields for $Re_0 = 10$ and $Re_o = 100$ retain these general behavior for the remaining of the droplet lifetime ($t = 9.9$).
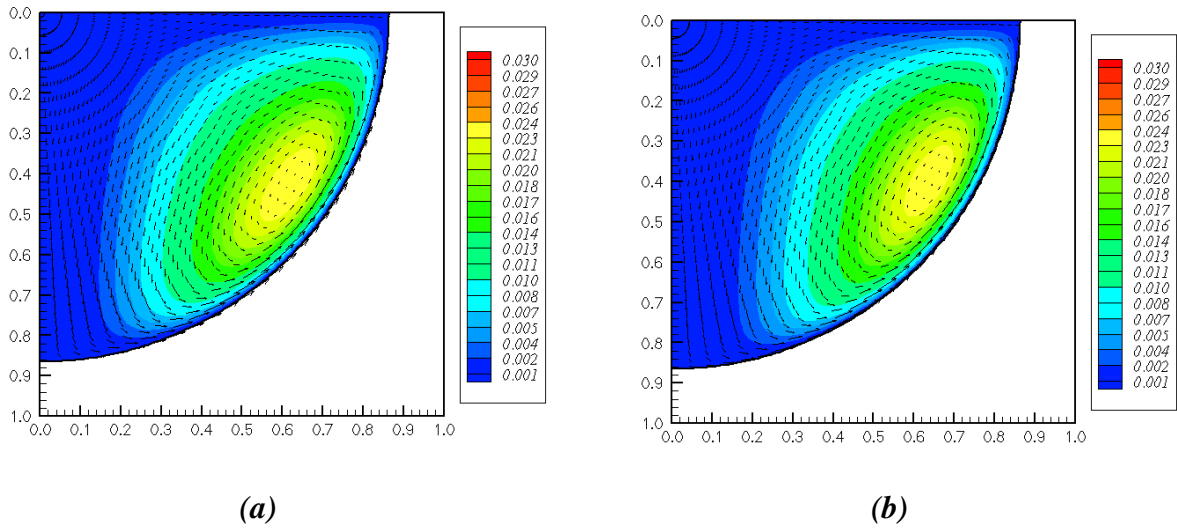

(a)   *(b)*

Figure 4. Stream-function and velocity vectors for $t = 3$, $Re_o = 10$ *(a)* and $Re_o = 100$ *(b)* – 126×126 grid, $\tau = 2.5$, $u_{\theta,s} = sin(2\theta)$, $u_r = 10^{-5}$

5. CONCLUSIONS

The numerical analysis of the transient convective effects inside liquid droplets in a linear infinite array was performed considering effects of droplet surface regression. Results, which show the importance of transient effects, are used to draw qualitative results of the flow and temperature development characteristics. The existence and development of two toroidal vortices, which contrasts with the single vortex structure found for isolated droplet in convective streams, is show to have a strong effect on the temperature field development. Besides, the influence of the droplet vaporization and the consequential liquid-gas interface regression is shown to have a lagging effect on the flow and temperature field developments. Further studies are necessary to quantify the droplet interaction with linear arrays of droplets considering gas and liquid transient behavior simultaneously.
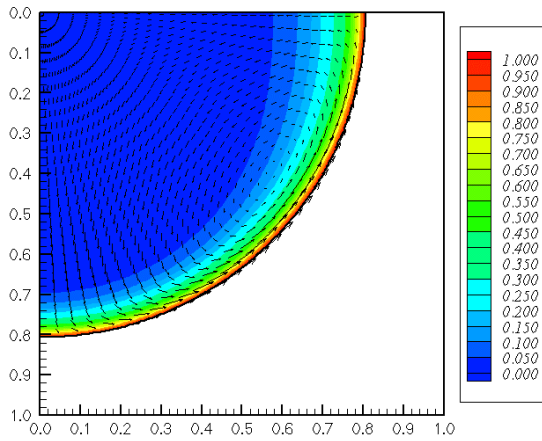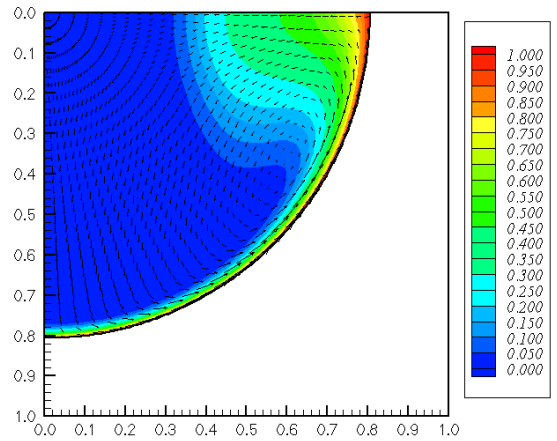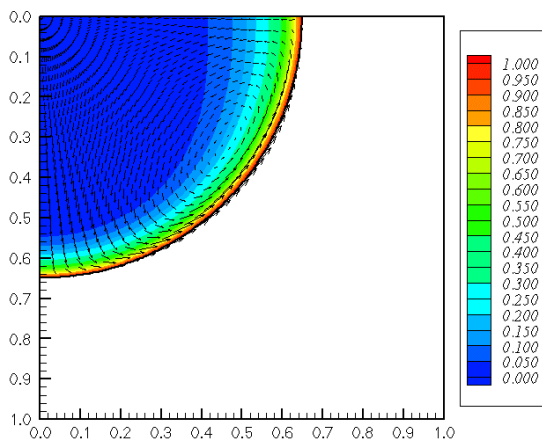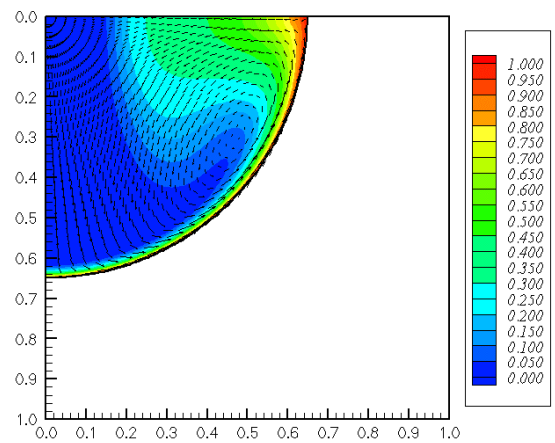
6. ACKNOWLEDGMENT
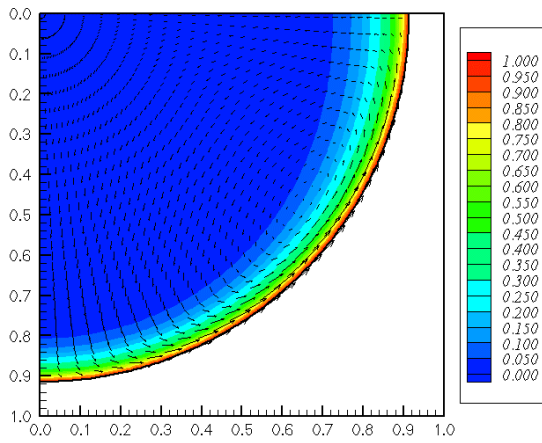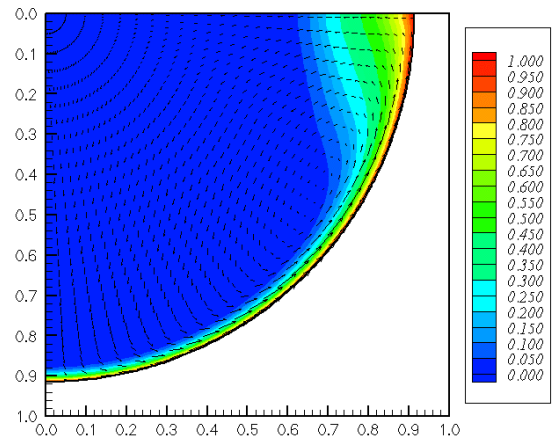
Figure 4. Temperature field and velocity vectors for $Re_o = 10 - t = 2$ **(a)**, $t = 4$ **(c)**, $t = 6$ **(e)** – and $Re_o = 100 - t = 2$ **(b)**, $t = 4$ **(d)**, $t = 6$ **(f)** – 126×126 Grid Points, $u_{\theta,s} = sin(2\theta), u_r = 10^{-5}$.

7. REFERENCES

- Anderson, D. A., Tannehill, J. C. and Pletcher, Richard H., 1984; "Computational Fluid Mechanics and Heat Transfer", Hemisphere Publishing Corporation.
- Annamalai, K, 1992.; "Interactive Process in Gasification and Combustion. Part I: Liquid Drop Arrays and Clouds", Progress Energy Combust. Science, Vol.18, pp.221-295.
- Hoffman, J. D. , 1992; "Numerical Methods for Engineers and Scientists", McGraw-Hill.
- Leiroz, A.J.K. and Rangel, R.H., 1995; "Numerical Study of Droplet-Stream Vaporization at Zero-Reynolds Number", Numerical Heat Transfer, Applications, Vol.27, pp.273-296.
- Leiroz, A.J.K. and Rangel, R.H. , 1995; "Interference Effects on Droplet Stream Comb.", Proc. 8th Int. Symp. on Transport. Phenomena in Combustion, San Francisco.
- Leiroz, A.J.K. , 1996; "Numerical Study of Droplet-Stream Vaporization and Combustion", Ph.D. Dissertation, University of California, Irvine.
- Moreira Filho, E.G. and Leiroz, A.J.K., 2000; "Numerical Study of Liquid Internal Circulation During Droplet-Stream Combustion", Brazilian Conference on Mechanical Engineering – CONEM 2000, Natal, RN, Brazil.
- Moreira Filho, E.G., 2000; "Analysis of Convective Effects Inside Liquid Droplets in Dense Linear Arrays", M.Sc. Dissertation, Instituto Militar de Engenharia, Rio de Janeiro, Brazil. (in Portuguese)
- Prakash S. and Sirignano W.A., 1978; "Liquid Fuel Droplet Heating with Internal Circulation", Int. Journal of Heat and Mass Transfer, Vol.21, 885-895.
- Prakash S. and Sirignano W.A, 1980; "Theory of Convective Droplet Vaporization with Unsteady Heat Transfer in the Circulating Liquid Phase", Int. Journal of Heat and Mass Transfer, Vol.23, 253-268.
- Rangel R.H. and Bian, X.,1995; "Numerical Solution of Inviscid Stagnation-Flow Solidification Problem", Numerical Heat Transfer, Part A, Vol. 28, pp. 589-603.
- Shih A.T. and Megaridis C.M., 1995; "Suspended Droplet Evaporation Modeling in a Laminar Convective Enviroment", Combustion and Flame, Vol. 102, pp. 256-270.
- Sirignano, W.A., 1993; "Fluid Dynamics of Sprays", Journal of Fluids Engineering., Vol.115, pp.345-378.
- Spalding, D.B., 1953; "The Combustion of Liquid Fuels", Proc. 4th International Symposium of Combustion, Cambridge, MA, pp. 847-864, Williams and Wilkins, Baltimore.
- Spalding, D.B. , 1955; "Some Fundamentals of Combustion", Butterworths, London.